NEUROLOGY/2018/940478

Title: Evidence for genetically determined degeneration of proprioceptive tracts in Friedreich ataxia

Running Title: Corticokinematic coherence in Friedreich ataxia

Authors: Brice Marty[1*], PhD & Gilles Naeije[1,2]*, MD, PhD; Mathieu Bourguignon[1,3,4], PhD; Vincent Wens[1,5], PhD; Veikko Jousmäki[6], PhD; David R Lynch[7], MD, PhD; William Gaetz[7], PhD; Serge Goldman[1], MD, PhD; Riitta Hari[8], MD, PhD; Massimo Pandolfo[2], MD, PhD; Xavier De Tiège[1,5], MD, PhD.

*These authors equally contributed to this study.

[1]Laboratoire de Cartographie fonctionnelle du Cerveau, ULB Neuroscience Institute, Université libre de Bruxelles (ULB), Brussels, Belgium.

[2]Department of Neurology, CUB Hôpital Erasme, Université libre de Bruxelles (ULB), Brussels, Belgium.

[3]Laboratoire Cognition Langage et Développement, ULB Neuroscience Institute, Université libre de Bruxelles (ULB), Brussels, Belgium.

[4]Basque Center on Cognition, Brain and Language (BCBL), Donostia, Spain.

[5]Department of Functional Neuroimaging, Service of Nuclear Medicine, CUB Hôpital Erasme, Université libre de Bruxelles (ULB), Brussels, Belgium.

[6]Department of Neuroscience and Biomedical Engineering, School of Science, Aalto University, Espoo, Finland.

[7]Children's Hospital of Philadelphia, Philadelphia, United States of America.

[8]Department of Art, Aalto University, Helsinki, Finland.

Corresponding author: Dr Gilles Naeije, Laboratoire de Cartographie fonctionnelle du Cerveau, ULB Neuroscience Institute, Université libre de Bruxelles (ULB), 808 Lennik Street, 1070 Brussels, Belgium. E-mail : Gilles.Naeije@erasme.ulb.ac.be.

Word count:

Title (characters) : 94

Abstract (words) : 219

Manuscript (words) : 3848

Fundings:

This study was financially supported by the research grant "Les Voies du Savoir" from the Fonds Erasme (Brussels, Belgium), the Fonds de la Recherche Scientifique (FRS-FNRS, Brussels, Belgium; research credit: J.0095.16.F), and a research grant from the Friedreich Ataxia Research Alliance (FARA, Drs Massimo Pandolfo, William Gaetz and David Lynch). Gilles Naeije was supported by a research grant from the Fonds Erasme (Brussels, Belgium). Mathieu Bourguignon was supported by the program Attract of Innoviris (grant 2015-BB2B-10), by the Spanish Ministry of Economy and Competitiveness (grant PSI2016-77175-P), and by the Marie Skłodowska-Curie Action of the European Commission (grant 743562). Xavier De Tiège and Gilles Naeije are Postdoctorate Clinical Master Specialist at the Fonds de la Recherche Scientifique (FRS-FNRS, Brussels, Belgium). The MEG project at the CUB Hôpital Erasme is financially supported by the Fonds Erasme (Research grant "Les Voies du Savoir", Brussels, Belgium). Accelerometer and PAM stimulator were designed and manufactured at Aalto NeuroImaging, Aalto University, Finland

Disclosures:

Dr. Naeije reports no disclosure.
Mr Marty reports no disclosure.
Mr Bourguignon reports no disclosure.
Mr Wens reports no disclosure.
Mr Jousmäki reports no disclosure.
Dr Lynch reports no disclosure.
Mr Gaetz reports no disclosure.
Dr Goldman reports no disclosure
Dr Hari reports no disclosure.
Dr Pandolfo reports no disclosure.
Dr De Tiège reports no disclosure.

Abstract

Objective: To assess using magnetoencephalography the developmental vs. progressive character of the impairment of spino-cortical proprioceptive pathways in Friedreich ataxia (FRDA).

Methods: Neuromagnetic signals were recorded from 16 right-handed FRDA patients (9 females, mean age: 27 y, mean scale for the assessment and rating of ataxia (SARA) score: 22.25) and matched healthy controls while they performed right finger movements either actively or passively. The coupling between movement kinematics (i.e., acceleration) and neuromagnetic signals was assessed using coherence at sensor and source levels. Such coupling, i.e., the corticokinematic coherence (CKC), specifically indexes proprioceptive afferent inputs to contralateral primary sensorimotor (cSM1) cortex. Non-parametric permutations and Spearman rank correlation test were used for statistics.

Results: In both groups of participants and movement conditions, significant coupling peaked at cSM1 cortex. Coherence levels were 70–75% lower in FRDA patients than in healthy controls in both movement conditions. In FRDA patients, coherence levels correlated with genotype alteration (i.e., the size of GAA1 triplet expansion) and the age of symptoms onset, but not with disease duration nor with SARA.

Conclusion: This study provides electrophysiological evidence demonstrating that proprioceptive impairment in FRDA is mostly genetically determined and scarcely progressive after symptoms onset. It also positions CKC as a reliable, robust and specific marker of proprioceptive impairment in FRDA.

Keywords: Friedreich ataxia, proprioception, cerebellum, magnetoencephalography, corticokinematic coherence.

Introduction

Friedreich ataxia (FRDA) is a rare autosomal recessive inherited ataxia mainly caused by expanded GAA triplet repeats in the first intron of the frataxin (FXN) gene (GAA1). GAA1 triplet expansion size correlates with age of onset and disease severity.[1] FRDA neuropathology affects dorsal root ganglia (DRG), posterior columns and spinocerebellar tracts in the spinal cord, followed by progressive atrophy of the cerebellar dentate nuclei and efferent fibers[2], leading to a "tabeto-cerebellar" ataxic pattern.[3]

Neuropathology and imaging studies show that DRG and spinal abnormalities occur very early and seem stable along time, leading to the onset and initial progression of ataxia.[4,5] However, DRG from patients with long disease duration still show signs of active inflammation, supporting a continuing degenerative process.[5] Dissecting the developmental from the progressive components of DRG and spinal pathology is therefore a critical issue for translational research in FRDA.[6]

Here, we used magnetoencephalography (MEG) and corticokinematic coherence (CKC) to answer that issue by objectively assessing the function of proprioceptive ascending pathways in FRDA. CKC indexes the coupling between cortical activity and movement kinematics (e.g., acceleration) during repetitive voluntary[7,8] and passive[9,10] movements. CKC is driven by movement-related proprioceptive afferents to contralateral primary sensorimotor (cSM1) cortex[10,11] and is relatively independent of movement rate.[12] Typically, CKC peaks at movement frequency and harmonics over cSM1 cortex.[7–10] We expected CKC levels at cSM1 cortex to be substantially reduced in FRDA patients and that they would correlate either with GAA1 triplet expansion size, age of disease onset, clinical scores, or disease duration.

Materials and methods

Participants

Sixteen FRDA patients (mean age 27 y, range 9–46 y; 9 females and 7 males; mean scale for the assessment and rating of ataxia (SARA) score: 21.4, range 9.5–30.5; mean GAA1 triplet expansion: 670, range 280–1000) and sixteen healthy controls (mean age 29 y; range 10–53 y; 9 females) without history of neuropsychiatric disease contributed to the study. Of note, one patient was heterozygous for a GAA1 repeat expansion and had a point mutation in the FXN gene.

Nine FRDA patients (mean age 36 y, range 23–46 y; 5 females; mean SARA score: 24, range 15.5–30.5, mean GAA1 triplet expansion: 621, range 280–910) also accepted to undergo somatosensory evoked potential (SEP) recording using electrical stimulation of the right median nerve. Recording and analysis of SEPs were done as in Santoro et al.[13] except that, for comfort reasons, the two trials consisted of 256 rather than 1000 epochs.

Ethical statement

All participants were included in the study after written informed consent. The study had prior approval by the CUB Hôpital Erasme Ethics Committee and was performed in accordance with the Declaration of Helsinki.

Experimental paradigm

The MEG experiment comprised three 5-min conditions (*Active*, *Passive*, and *Rest)* that were randomized across participants.

Figure 1 illustrates the two movement conditions used in this study.

In *Active*, participants performed repetitive right index finger–thumb oppositions at a regular rate (about 2 Hz). Pauses were introduced if necessary.

In *Passive*, a pneumatic artificial muscle (PAM) stimulator adapted from Piitulainen et al.[11] induced passive flexion–extensions of participants' right index finger at 3 Hz. This stimulator consisted of an elastic PAM (DMSP-10-100 AM-CM, Festo AG & Co, Esslingen, Germany) inserted horizontally in a polyoxymethylene cylinder on which participants could rest their hand. The PAM moved in the horizontal direction (5 mm of displacement) when its internal air pressure was varied (0–4 bar). The pressure was regulated by a solenoid valve (SY5220-6LOU-01F-Q, SMC Corporation, Tokyo, Japan) that was controlled by the internal MEG-stimulator system.

In *Active* and *Passive* conditions, participants' finger movements were monitored with a 3-axis accelerometer (Acc, ADXL335 iMEMS Accelerometer, Analog Devices, Inc., Norwood, MA, USA) attached to the nail of their right index finger.

In *Rest,* participants were instructed to relax and not to move.

In all conditions, participants were instructed to gaze at a fixation point in the magnetically shielded room (MSR) to avoid any eye movements or visual perception of the moving finger. They also wore earplugs to block the noise generated by finger movements or the PAM stimulator.

— Place Figure 1 about here —

Data acquisition

MEG signals were recorded with a whole-scalp-covering neuromagnetometer placed in a light-weight MSR (Vectorview & Maxshield™ (Elekta Oy, Helsinki, Finland) for 10 patients and 4 control individuals, and its upgraded version with similar sensor layout, the Triux & Maxshield™ (MEGIN, Helsinki, Finland), for 6 patients and 12 control individuals). MEG signals were filtered at 0.1–330 Hz and sampled at 1 kHz. Four head-tracking coils were used to monitor participants' head position inside the MEG helmet. The locations of the coils and at least 200 head-surface points (on scalp, nose, and face) with respect to anatomical fiducials were determined with an electromagnetic tracker (Fastrak, Polhemus, Colchester, VT, USA) prior to MEG data acquisition. Acc signals were recorded time-locked to MEG using a lowpass at 330 Hz and a sampling rate of 1 kHz. High-resolution 3D-T1 cerebral magnetic resonance images (MRIs) were acquired on a 1.5 T MRI scanner (Intera, Philips, The Netherlands). Both MEG and MRI data were acquired at the CUB Hôpital Erasme.

Data preprocessing

Continuous MEG data were first preprocessed off-line using the signal space separation method[14] to suppress external interferences and correct for head movements. Acceleration signal was computed at every time sample as the Euclidian norm of the three band-passed Acc channels. Both MEG and Acc signals were split into 2-s epochs with 1.5-s overlap, leading to a spectral resolution of 0.5 Hz.[15] Epochs within which the amplitude of MEG signals filtered through 0.1–145 Hz exceeded 3 pT (magnetometers) or 0.7 pT/cm (gradiometers) were marked as artifact-contaminated and rejected from further analysis. This procedure led to a similar

amount of epochs (FRDA patients: *Active* 665 ± 126 (mean ± SD), *Passive* 667 ± 160; healthy controls: *Active* 755 ± 52, *Passive* 655 ± 180) between conditions (ANOVA, *Active* vs. *Passive*; $F_{1,15} = 1.09$, $p = 0.44$) and groups of participants (ANOVA, FRDA patients vs. healthy controls $F_{2,30} = 1.38, p = 0.26$) .

Movement regularity

Movement regularity was quantified in the *Active* condition for all participants. The principal component of the three high-passed (0.5 Hz) Acc signals was computed and then Fourier transformed. The resulting power spectrum was then smoothed with a Gaussian kernel (full width at half maximum (FWHM) 0.3 Hz). The first peak of the spectrum curve was then identified and its FWHM was estimated. The former provided an estimate of movement frequency, and the latter, an indicator of movement regularity (i.e., the smaller its value, the more regular the movements), at least under the hypothesis of movement stationarity. However, self-paced movement may present nonstationary drifts in movement frequency over the whole recording session while still being regular on the short term. Therefore, the global regularity index may lead to a false indication of irregularity. To take this possibility into account, we also estimated a "short-time measure" of regularity by computing the above FWHM index within 10 s-wide sliding windows and then averaging it over all windows.

Coherence analyses between Acc and MEG signals in sensor space

Coherence quantifies the degree of coupling between two signals by providing a number between 0 (no linear dependency) and 1 (perfect linear dependency) for each frequency.[16] For each movement condition (*Active, Passive*), coherence between Acc

and MEG signals was computed in sensor space as in [7,10,17] to identify, without any *a priori*, the frequencies showing significant coupling between those signals. Frequencies showing consistent coherence across participants in sensor space were then defined as *frequencies of interest* for source-level analyses.

Coherence analyses in source space

MEG forward models and individual-level coherence maps were then computed in source space following a procedure detailed in previous studies from our group[35,38,39] to obtain normalized coherence maps in the MNI space for each participant, condition (*Active, Passive*), and frequency of interest. Coherence maps at the group level were subsequently produced.[35,38,39]

Statistical analyses

Sensor-space coherence at individual level

The statistical significance of individual coherence levels was assessed under the hypothesis of linear independence.[16] The significance threshold (*Ct*) is given by

$$Ct = 1 - p^{1/(L-1)}$$

where p is the chosen significance level for individual channels and L, the number of disjoint epochs used for coherence estimation. The significance level was set to $p < 0.05$ Bonferroni corrected for multiple comparisons (i.e., 306 channels).

Statistical differences in movement frequency, movement regularity and coherence levels in sensor space

Differences in movement frequency (*Active, Passive*) and regularity (*Active*) between groups of participants (FRDA patients vs. healthy controls) were assessed

using a 2-sample *t*-test. The effects of group of participants, movement conditions, and frequencies of interest on maximal sensor-level coherence were assessed with 3-way repeated-measures ANOVA. Results were considered statistically significant at $p < 0.05$.

Source-space coherence at the group level

Statistical significance of local coherence maxima, identified in group-level coherence maps for each movement condition and frequency of interest, was assessed with a non-parametric permutation test[18], following the procedure described in[7]. Statistical differences in group-level coherence maps in *Active* and *Passive* between healthy controls and FRDA patients were assessed for each frequency of interest with a similar non-parametric permutation test as those previously described[7], with the only difference that group-level difference maps were obtained by subtracting healthy controls' Fisher-transformed *Active* or *Passive* coherence maps with the corresponding FRDA patients' coherence maps.

Correlation analyses of individual source-space coherence values

Spearman rank correlation tests were used to seek for possible relations between FRDA patients' maximum coherence levels at cSM1 cortex for each frequency of interest and the size of GAA1 triplet expansion, SARA score, age of onset of clinical symptoms, and disease duration. Of note, the patient with point mutation in the FXN gene was excluded from the correlations with GAA1 triplet expansion. Results were considered statistically significant at $p < 0.05$.

Data availability statement

De-identified participants' data will be shared as well as study protocol and statistical analyses upon request.

Results

Active condition

Despite identical instructions, FRDA patients moved at a slower pace and less regularly than healthy controls (movement frequency (F0): 1.75 ± 0.5 Hz vs. 2.60 ± 1 Hz, $p = 0.03$; stationary movement regularity: 1.20 ± 1.10 Hz vs 0.64 ± 0.35 Hz, $p = 0.084$; short-time regularity: 0.59 ± 0.14 Hz vs 0.49 ± 0.07 Hz; $p = 0.016$).

Coherence at the sensor level

Table 1 and Figure 2 summarize sensor-level coherence results obtained in both groups of participants and movement conditions.

Statistically significant coherence peaked at F0 and its first harmonics (F1) in all healthy controls in the *Active* condition, and in all (F0) and 15/16 (F1) of them in the *Passive* condition. All FRDA patients displayed a significant coherence peak at F0, while 15/16 of them presented a significant coherence peak at F1 in the *Active* condition. In the *Passive* condition, significant coherence was found in 14/16 of FRDA patients at F0 and in 8/16 of them at F1. In both groups of participants and conditions, coherence was maximal at central sensors contralateral to hand movements.

— Place Table 1 about here —

The 3-way ANOVA conducted on maximal sensor level coherence disclosed a main effect of frequency of interest ($F_{1,15}$ = 17.2, p = 0.001), movement condition ($F_{1,15}$ = 27.2, p = 0.0001), and participants' group ($F_{1,15}$ = 20.3, p < 0.0001), and an interaction between frequency of interest and movement condition ($F_{1,15}$ = 10.5, p = 0.006) and no other significant interaction ($F_{1,15}$ < 0.70, p > 0.77). This pattern of results was explained by higher CKC values in healthy controls compared with FRDA patients, and lower CKC values at F1 than at F0 in *Passive*. Based on sensor-level coherence results, only F0 and F1 were considered for further source-space analyses.

— Place Figure 2 about here —

Coherence at the source level

To identify the neuronal networks involved in coherence in *Active* and *Passive* conditions, similar coherence analyses were performed at the frequencies of interest (i.e., F0 and F1) at the source level. Figure 3 illustrates the results.

Active condition

In healthy controls, significant F0 and F1 coherence occurred at cSM1 cortex with maximal amplitude over the hemisphere contralateral to hand movements (F0, MNI peak coordinates: [–44 –21 58] mm, coherence value: 0.40; F1, [–43 –23 60], 0.38). Of note, a clear but non-significant local coherence maximum was also observed at the ipsilateral SM1 (iSM1) cortex ([42 –31 56], 0.10). In FRDA patients, significant F0 coherence occurred at bilateral SM1 cortices with maximal amplitude over the hemisphere contralateral to hand movements (cSM1 cortex, [–41 –18 60], 0.10; iSM1 cortex, [34 –18 65], 0.08). Significant F1 coherence was also only found

at cSM1 cortex ([–45 –22 57], 0.10). Coherence at F0 and F1 over cSM1 cortex (F0, [–48 –29 56]; F1, [–36 –17 64]) was significantly higher in healthy controls than FRDA patients (F0: 0.4 vs 0.10; F1: 0.38 vs ??0.08??).

Passive condition

In healthy controls and FRDA patients, significant F0 and F1 coherence occurred at cSM1 cortex (healthy controls, F0: [–45 –21 58], 0.3/F1: [–47 –25 57], 0.10; FRDA patients, F0: [–48 –19 54], 0.10/F1: [–49 –20 51], 0.04). At F0, coherence levels at cSM1 cortex were significantly lower in FRDA patients compared with healthy controls (F0: [–33 –14 68], 0.10 vs 0.30), while no significant difference was observed at F1.

— Place Figure 3 about here —

Correlation analyses

In FRDA patients with GAA1 triplet expansion (15/16 FRDA patients), levels of cSM1 cortex coherence in *Active* F1 correlated with the age of onset ($r = 0.75$, $p = 0.004$) and with the size of GAA1 triplet expansion ($n = 15$; $r = –0.67$, $p = 0.001$). In *Passive*, levels of F1 cSM1 cortex coherence correlated only with the size of GAA1 triplet expansion ($n = 15$; $r = –0.59$, $p = 0.009$). No other correlation appeared significant. Figure 4 illustrates those correlations.

— Place Figure 4 about here —

SEPs

N20 response was clearly identified in only 2/9 of the FRDA patients who underwent classical SEP testing, with latencies of 26.1 ms and 27.7 ms, and amplitudes of 0.3 □V and 0.4 □V (normal values of the Clinical Neurophysiology Department of the CUB Hôpital Erasme for N20 latency and amplitude: 19.6 ± 1.0 ms and 2.1 ± 0.9 □V respectively).

Discussion

This study demonstrates that (i) the coupling between index-finger movement kinematics and cSM1 cortex neuromagnetic activity is reduced in FRDA patients compared with healthy controls matched for age and sex during both active and passive finger movements, (ii) CKC is a more reliable measure than SEPs in FRDA patients, and (iii) the level of coherence at cSM1 cortex in FRDA patients correlates with the size of GAA1 triplet expansion in both *Active* and *Passive* at F1, but not with the SARA score or disease duration. These findings provide empirical evidence supporting that the severity of spino-cortical proprioceptive pathways degeneration in FRDA is genetically determined and has little tendency to progress after disease onset. They also validate CKC as a specific and robust electrophysiological marker of spino-cortical proprioceptive pathways degeneration in FRDA.

Previous CKC studies performed in healthy controls demonstrated that CKC is robustly observed at cSM1 cortex at the individual level during both active[7,8,17] and passive[10,11] finger movements. Furthermore, they highlighted that CKC is driven by movement-related proprioceptive afferent input to cSM1 cortex with negligible influence of tactile input.[10,11] A longitudinal study performed in a similar population

also demonstrated that CKC levels at cSM1 cortex are fairly reproducible across sessions.[19] All these findings set the rationale for using CKC to obtain an objective, reliable, and specific measure of proprioceptive pathways impairment in FRDA patients. The working hypothesis guiding the present study was that the use of CKC would bring novel insights into FRDA pathophysiology and, more particularly, into the developmental vs. the degenerative character of proprioceptive pathways impairment in this disorder.

As expected, in both *Active* and *Passive* conditions, CKC levels were substantially decreased in FRDA patients (decrease by about a third or a quarter of the values in healthy controls). Furthermore, a negative correlation was found in both movement conditions between CKC levels at F1 and the size of GAA1 triplet expansion. These findings therefore imply that the low CKC levels observed in FRDA patients are actually the consequence of an early and scarcely progressive, possibly developmental, pathology of spino-cortical proprioceptive pathways. These results also imply that whenever genetic therapy to restore DRG and medullary posterior columns FXN level becomes available, it should be started as early as possible at the preclinical stage. Yet, an early proprioceptive pathology, possibly even hypoplasia, does not imply that the remaining somatosensory neurons responsible for residual proprioception in FRDA patients would not degenerate with time and contribute to the progressive worsening of ataxia. However, CKC data indicate that, in the course of FRDA, the ongoing loss of proprioception is likely to be minor compared with cerebellar and pyramidal degenerations.[2,20] Longitudinal CKC investigations along the course of FRDA could help to clarify the existence of subtle progressive dysfunction of the posterior column and to assess the potential yield of early therapeutic intervention to alleviate symptoms of the proprioceptive impairment. Still,

the lack of correlation of CKC levels at cSM1 cortex and disease duration does not support this hypothesis.

Previous studies have demonstrated that SEPs are not reliably identified between 1/3 and 2/3 of FRDA patients.[13,21–26] Our finding that SEPs were visible only in 2/9 FRDA patients is in line with those data. In the Naples cohort[15] where SEPs were detectable in 36 out of 52 patients, FRDA patients had similar GAA1 repeat expansions (621 ± 225 for CUB Hôpital Erasme vs. 661 ± 257 for Naples) but different disease durations (20 ± 11 years vs. 10 ± 7 years). However, the difference in disease duration is not likely to account for the discrepancy between our rates of recordable SEPs as, in the Naples cohort, N20 amplitude did not correlate with disease duration. A possible explanation for the better sensitivity of SEPs in the Naples cohort could be that, to record SEPs, they averaged the neural responses elicited by 2000 electrical stimuli on each side[15], while we limited the number of electrical stimuli on each side to 512 meaning that their signal-to-noise ratio was 2 times ours. Still, despite the frequent absence of SEPs in FRDA patients, CKC was reliably recorded in all (*Active*) or almost all (*Passive*) patients, even when SEPs were not detectable. Interestingly, when measurable, the amplitude of N20 responses obtained in previous studies tended to be stable over time and correlated with the size of GAA1 triplet expansion, while the correlation with disease progression varied across studies.[13,22–25,27] These findings indicate that the loss of N20 and the reduction of CKC levels share similar disease-related impairment of the somatosensory system. However, as CKC can be measured in almost all FRDA patients, it appears as a robust, more reliable and specific marker than SEP recordings to assess the pathology of proprioceptive pathways in FRDA. FRDA patients who are compound heterozygotes (GAA expansion and a *FXN* point mutation) display the same mixed

afferent and cerebellar ataxia phenotype than homozygous GAA triplet expansion FRDA patients[28], so CKC can be used to assess spino-cortical proprioceptive pathways alteration in these patients as well. Results also suggest that CKC could be of great interest to assess impairment of proprioceptive pathways in various diseases affecting the posterior columns of the spinal cord, such as multiple sclerosis[29], vitamin B12 deficiency[30], stroke[31], and medullary compression.[32] Such studies would also inform about the specificity of the CKC alterations in different patient groups, including FRDA. Finally, in FRDA and other genetic spinocerebellar ataxias (SCAs), CKC could potentially serve to identify preclinical stages in patients in whom a genetic diagnosis was made. Indeed, in most common SCAs (1, 2, 3 & 6) and in FRDA, genotypic anomalies only predict a part of age-of-onset variability, disease severity, and survival.[33,35] On the other hand, in SCAs, SEPs are altered as early as eight years before symptoms onset (for a review, see[36]), which suggests that CKC, as a robust method, might help to sort pre-symptomatic patients and therefore play a role in the determination of the optimum time for early therapeutic intervention.

That FRDA patients moved at a slower pace and less regularly than healthy controls in the *Active* condition is unlikely to explain the difference in CKC levels observed between the two groups. Indeed, CKC levels in *Active* and *Passive* conditions were similar at F0 in both groups of participants and stronger in the *Active* condition at F1 in FRDA patients. This (expectable) difference in movement characteristics between FRDA patients and healthy controls justifies the importance of the *Passive* condition. The interest of the use of a metronome to pace active movements should be addressed in future studies. In *Active* and *Passive* conditions, CKC peaked at F0 and F1 over cSM1 cortex in both groups of participants, which is in line with previous CKC studies performed in healthy individuals.[7,9,10] Our finding

that, in the *Active* condition, local CKC maxima at iSM1 cortex were significant only in FRDA patients is explained by the statistical approach used in this study. Indeed, permutation tests may be too conservative (type II error) for voxels other than those with high coherence levels.[18] In FRDA patients, CKC levels at cSM1 cortex were much lower than those observed in healthy controls, explaining why CKC levels at iSM1 cortex appeared significant in FRDA patients and not in healthy controls.

The neural bases of CKC at F0 and F1 are still debated. F0 and F1 CKC may either reflect cortical processing of different movement kinematics features, or F1 may be due to non-sinusoidal cortical activity at F0, leading to coherence at twice F0.[7] In repetitive index-finger movements, such as those used in this study, F0 is likely to reflect cycles of index finger flexions/extensions and corresponding proprioceptive signals, while F1 might reflect the contraction/relaxation of agonist and antagonist muscles during both flexion and extension. This difference between F0 and F1 CKC might explain why FRDA patients' CKC levels at cSM1 cortex correlated with the size of GAA1 triplet expansion and the age of onset better at F1 than at F0. Also, the absence of significant difference between healthy controls and FRDA patients at F1 in the *Passive* condition are probably related to the relatively weak coherence at F1 observed in healthy controls and to the variability of this frequency in FRDA patients.

In conclusion, FRDA is a complex neurogenetic disorder that mainly involves degeneration of proprioceptive afferent and cerebellar pathways. Clinical rating scales are able to capture the progression of cerebellar impairment, but the involvement of proprioceptive pathways is less well quantified clinically, hence the need for robust markers of proprioceptive impairment. We provided electrophysiological evidence that spino-cortical proprioceptive impairment in FRDA is mostly genetically

determined and scarcely progressive after symptoms onset. We also demonstrate that CKC represents a reliable and robust individual-level marker of spino-cortical proprioceptive loss in FRDA. CKC may therefore represent a useful addition to the armamentarium of FRDA clinical evaluation to assess the natural history of this disorder and the efficacy of dedicated early therapeutic approaches.

Appendix 1

Name	Location	Role	Contribution
Gilles Naeije, MD, PhD	Université libre de Bruxelles (ULB), Brussels, Belgium	Author	Designed and conceptualized study; conducted the experiments; analyzed the data; wrote the manuscript; designed Figure 4; wrote the revisions.
Brice Marty, PhD	Université libre de Bruxelles (ULB), Brussels, Belgium	Author	Conducted the experiments; analyzed the data; contributed to the writing of Methods, Results, and Figures 1-3 legends; designed Figures 1-3.
Mathieu Bourguignon, PhD	Université libre de Bruxelles (ULB), Brussels, Belgium	Author	Analyzed the data; drafted the manuscript for intellectual content.
Vincent Wens, PhD	Université libre de Bruxelles (ULB), Brussels, Belgium	Author	Analyzed the data; drafted the manuscript for intellectual content.
Veikko Jousmäki, PhD	School of Science, Aalto University, Espoo, Finland	Author	Designed and provided the PAM stimulator; provided input for research design and interpretation; drafted the manuscript for intellectual content.
David R Lynch, MD, PhD	Children's Hospital of Philadelphia, Philadelphia, USA	Author	Drafted the manuscript for intellectual content.
William Gaetz, PhD	Children's Hospital of Philadelphia, Philadelphia,	Author	Provided input for research design and interpretation; drafted the

	USA		manuscript for intellectual content.
Serge Goldman, MD, PhD	Université libre de Bruxelles (ULB), Brussels, Belgium	Author	Drafted the manuscript for intellectual content; provided input for research design and interpretation.
Riitta Hari,MD, PhD	Department of Art, Aalto University, Helsinki, Finland	Author	Drafted the manuscript for intellectual content; provided input for research design and interpretation.
Massimo Pandolfo, MD, PhD	Université libre de Bruxelles (ULB), Brussels, Belgium	Author	Designed and conceptualized the study; drafted the manuscript for intellectual content; provided input for research design and interpretation.
Xavier De Tiège, MD, PhD	Université libre de Bruxelles (ULB), Brussels, Belgium	Author	Designed and conceptualized the study; wrote the manuscript; drafted the manuscript for intellectual content; provided input for research design and interpretation; contributed to the revisions.

References

1. Campuzano V, Montermini L, Molto MD, et al. Friedreich's ataxia: autosomal recessive disease caused by an intronic GAA triplet repeat expansion. Science. 1996;271(5254):1423-1427.
2. Koeppen AH, Mazurkiewicz JE. Friedreich Ataxia: Neuropathology Revised. J Neuropathol Exp Neurol. 2013;72(2):78-90. doi:10.1097/nen.0b013e31827e5762
3. Pandolfo M. Friedreich Ataxia. Arch Neurol. 2008;65(10). doi:10.1001/archneur.65.10.1296
4. Mascalchi M, Bianchi A, Ciulli S, et al. Lower medulla hypoplasia in Friedreich ataxia: MR Imaging confirmation 140 years later. J Neurol. 2017;264(7):1526-1528. doi:10.1007/s00415-017-8542-8
5. Koeppen AH, Ramirez RL, Becker AB, Mazurkiewicz JE. Dorsal root ganglia

in Friedreich ataxia: satellite cell proliferation and inflammation. Acta Neuropathol Commun. 2016;4(1):46. doi:10.1186/s40478-016-0288-5

6. Piguet F, de Montigny C, Vaucamps N, Reutenauer L, Eisenmann A, Puccio H. Rapid and Complete Reversal of Sensory Ataxia by Gene Therapy in a Novel Model of Friedreich Ataxia. Mol Ther. May 2018. doi:10.1016/j.ymthe.2018.05.006

7. Bourguignon M, Jousmäki V, Op de Beeck M, Van Bogaert P, Goldman S, De Tiège X. Neuronal network coherent with hand kinematics during fast repetitive hand movements. Neuroimage. 2012;59(2):1684-1691. doi:10.1016/j.neuroimage.2011.09.022

8. Piitulainen H, Bourguignon M, De Tiège X, Hari R, Jousmäki V. Coherence between magnetoencephalography and hand-action-related acceleration, force, pressure, and electromyogram. Neuroimage. 2013;72:83-90. doi:10.1016/j.neuroimage.2013.01.029

9. Bourguignon M, Piitulainen H, De Tiège X, Jousmäki V, Hari R. Corticokinematic coherence mainly reflects movement-induced proprioceptive feedback. Neuroimage. 2015;106:382-390. doi:10.1016/j.neuroimage.2014.11.026

10. Piitulainen H, Bourguignon M, De Tiège X, Hari R, Jousmäki V. Corticokinematic coherence during active and passive finger movements. Neuroscience. 2013;238:361-370. doi:10.1016/j.neuroscience.2013.02.002

11. Piitulainen H, Bourguignon M, Hari R, Jousmäki V. MEG-compatible pneumatic stimulator to elicit passive finger and toe movements. Neuroimage. 2015;112:310-317. doi:10.1016/j.neuroimage.2015.03.006

12. Marty B, Bourguignon M, Op de Beeck M, et al. Effect of movement rate on

corticokinematic coherence. Neurophysiol Clin Neurophysiol. 2015;45(6):469-474. doi:10.1016/j.neucli.2015.09.002

13. Santoro L, Perretti A, Lanzillo B, et al. Influence of GAA expansion size and disease duration on central nervous system impairment in Friedreich's ataxia: contribution to the understanding of the pathophysiology of the disease. Clin Neurophysiol. 2000;111(6):1023-1030. doi:10.1016/s1388-2457(00)00290-x

14. Taulu S, Simola J, Kajola M. Applications of the signal space separation method. Signal Process IEEE …. 2005. doi:10.1109/TSP.2005.853302

15. Bortel R, Sovka P. Regularization Techniques in Realistic Laplacian Computation. IEEE Trans Biomed Eng. 2007. doi:10.1109/TBME.2007.893496

16. Halliday DM, Rosenberg JR, Amjad AM, Breeze P, Conway BA, Farmer SF. A framework for the analysis of mixed time series/point process data--theory and application to the study of physiological tremor, single motor unit discharges and electromyograms. Prog Biophys Mol Biol. 1995;64(2-3):237-278.

17. Marty B, Bourguignon M, Jousmäki V, et al. Cortical kinematic processing of executed and observed goal-directed hand actions. Neuroimage. 2015;119:221-228. doi:10.1016/j.neuroimage.2015.06.064

18. Nichols TE, Holmes AP. Nonparametric permutation tests for functional neuroimaging: A primer with examples. Hum Brain Mapp. 2002. doi:10.1002/hbm.1058

19. Piitulainen H, Illman M, Laaksonen K, Jousmäki V, Forss N. Reproducibility of corticokinematic coherence. Neuroimage. 2018;179:596-603. doi:10.1016/j.neuroimage.2018.06.078

20. Cruz-Martínez A, Palau F, Cruz-Martinez A, Palau F. Central motor conduction time by magnetic stimulation of the cortex and peripheral nerve conduction follow-up studies in Friedreich's ataxia. Electroencephalogr Clin Neurophysiol. 1997;105(6):458-461. doi:10.1016/s0924-980x(97)00047-7

21. Santiago-Perez S, Perez-Conde MC, Ugalde-Canitrot A, Lopez-Pajares MR. A neurophysiological study of the alterations to the central and peripheral nervous systems in Friedreich's ataxia. Rev Neurol. 2007;44(4):193-197.

22. Santoro L, De Michele G, Perretti A, et al. Relation between trinucleotide GAA repeat length and sensory neuropathy in Friedreich's ataxia. J Neurol Neurosurg Psychiatry. 1999;66(1):93-96. doi:10.1136/jnnp.66.1.93

23. Vanasse M, Garcia-Larrea L, Neuschwander P, Trouillas P, Mauguière F. Evoked Potential Studies in Friedreich's Ataxia and Progressive Early Onset Cerebellar Ataxia. Can J Neurol Sci / J Can des Sci Neurol. 1988;15(03):292-298. doi:10.1017/s0317167100027773

24. Ouvrier RA, McLeod JG, Conchin TE. Friedreich's ataxia. Early detection and progression of peripheral nerve abnormalities. J Neurol Sci. 1982;55(2):137-145.

25. Pelosi L, Fels A, Petrillo A, et al. Friedreich's ataxia: clinical involvement and evoked potentials. Acta Neurol Scand. 1984;70(5):360-368. doi:10.1111/j.1600-0404.1984.tb00837.x

26. Jones SJ, Baraitser M, Halliday AM. Peripheral and central somatosensory nerve conduction defects in Friedreich's ataxia. J Neurol Neurosurg Psychiatry. 1980;43(6):495-503. doi:10.1136/jnnp.43.6.495

27. Santoro L, Perretti A, Crisci C, et al. Electrophysiological and histological follow-up study in 15 Friedreich's ataxia patients. Muscle Nerve.

1990;13(6):536-540. doi:10.1002/mus.880130610

28. Cossée M, Dürr A, Schmitt M, et al. Friedreich's ataxia: point mutations and clinical presentation of compound heterozygotes. Ann Neurol. 1999;45(2):200-206. http://www.ncbi.nlm.nih.gov/pubmed/9989622. Accessed January 3, 2019.

29. Ganes T. Somatosensory evoked responses and central afferent conduction times in patients with multiple sclerosis. J Neurol Neurosurg Psychiatry. 1980;43(10):948-953.

30. Zegers de Beyl D, Delecluse F, Verbanck P, Borenstein S, Capel P, Brunko E. Somatosensory conduction in vitamin B12 deficiency. Electroencephalogr Clin Neurophysiol. 1988;69(4):313-318.

31. Tinazzi M, Mauguiere F. Assessment of intraspinal and intracranial conduction by P30 and P39 tibial nerve somatosensory evoked potentials in cervical cord, brainstem, and hemispheric lesions. J Clin Neurophysiol. 1995;12(3):237-253.

32. Miyoshi T, Kimura J. Short-latency somatosensory evoked potentials in patients with cervical compressive lesions: morphological versus functional examination. Electromyogr Clin Neurophysiol. 1996;36(6):323-332.

33. Schmitz-Hubsch T, du Montcel ST, Baliko L, et al. Scale for the assessment and rating of ataxia: Development of a new clinical scale. Neurology. 2006;66(11):1717-1720. doi:10.1212/01.wnl.0000219042.60538.92

34. van de Warrenburg BPC, Hendriks H, Dürr A, et al. Age at onset variance analysis in spinocerebellar ataxias: A study in a Dutch-French cohort. Ann Neurol. 2005;57(4):505-512. doi:10.1002/ana.20424

35. Reetz K, Dogan I, Costa AS, et al. Biological and clinical characteristics of the European Friedreich's Ataxia Consortium for Translational Studies (EFACTS)

cohort: a cross-sectional analysis of baseline data. Lancet Neurol. 2015;14(2):174-182. doi:10.1016/S1474-4422(14)70321-7

36. Maas RPPWM, van Gaalen J, Klockgether T, van de Warrenburg BPC. The preclinical stage of spinocerebellar ataxias. Neurology. 2015;85(1):96-103. doi:10.1212/WNL.0000000000001711

Legends of the figures

Figure 1

Movement conditions. **Top.** *Passive* condition. Illustration of the passive movements of the right index finger induced by the Pneumatic Artificial Muscle (PAM) stimulator. During the experiments, the right index finger was taped to the moving extremity of the PAM stimulator. **Bottom.** One movement cycle of the right index finger and thumb in *Active* condition. An accelerometer was attached to the right index finger nail in both conditions.

Figure 2

Individual coherence spectra for each participant and movement condition (**Top**, *Active*; **Bottom**, *Passive*). Each gray trace represents the coherence between MEG and accelerometer signals for a single individual. For each frequency bin, the coherence value displayed is the maximum coherence across the MEG sensors covering the left rolandic MEG sensors. Black traces are group averages. Frequencies are expressed in F0 units (i.e., 1 corresponds to the individual F0, 2 to its F1, etc.).

Figure 3

Group-level coherence maps superimposed on brain surface rendering. All maps are thresholded at statistically significant coherence level (lower bound of the color scale, permutation-based statistics). The brain is viewed from the top. Group-level coherence maps for healthy controls (**Top**) and FRDA patients (**Middle**) in *Active* (**Left**) and *Passive* (**Right**) conditions at movement frequency (F0) and its first harmonics (F1). **Bottom.** Difference in group-level coherence maps between healthy controls and FRDA patients in *Active* (**Left**) and *Passive* (**Right**) conditions at F0 and

F1.

Figure 4

Plot of the Spearman correlation between FRDA patients' individual CKC levels at F1 in the *Active* condition and the size of GAA1 triplet expansion on the shortest allele (nGAA1) (**Left**) or the age of onset (**Middle**), and between FRDA patients' individual CKC levels at F1 in the *Passive* condition and the size of GAA1 triplet expansion on the shortest allele (nGAA1) (**Right**). Of note, when the two patients with the shortest GAA1 who are associated with the highest CKC values at F1 are removed from the analyses, correlations remain (nGAA1, *Active:* r = -0.66/p = 0.014, *Passive*: r = -0.56/p = 0.047; age of onset, *Active:* r= 0.56/p = 0.047*)*

Table 1: Maximal coherence level at rolandic MEG sensors contralateral to finger movements

	Maximal coherence level (mean ± SD)			
	Active		*Passive*	
	F0	F1	F0	F1
Healthy controls	0.39 ± 0.18	0.40 ± 0.18	0.32 ± 0.18	0.13 ± 0.08
FRDA patients	0.12 ± 0.08	0.11 ± 0.12	0.14 ± 0.14	0.06 ± 0.08

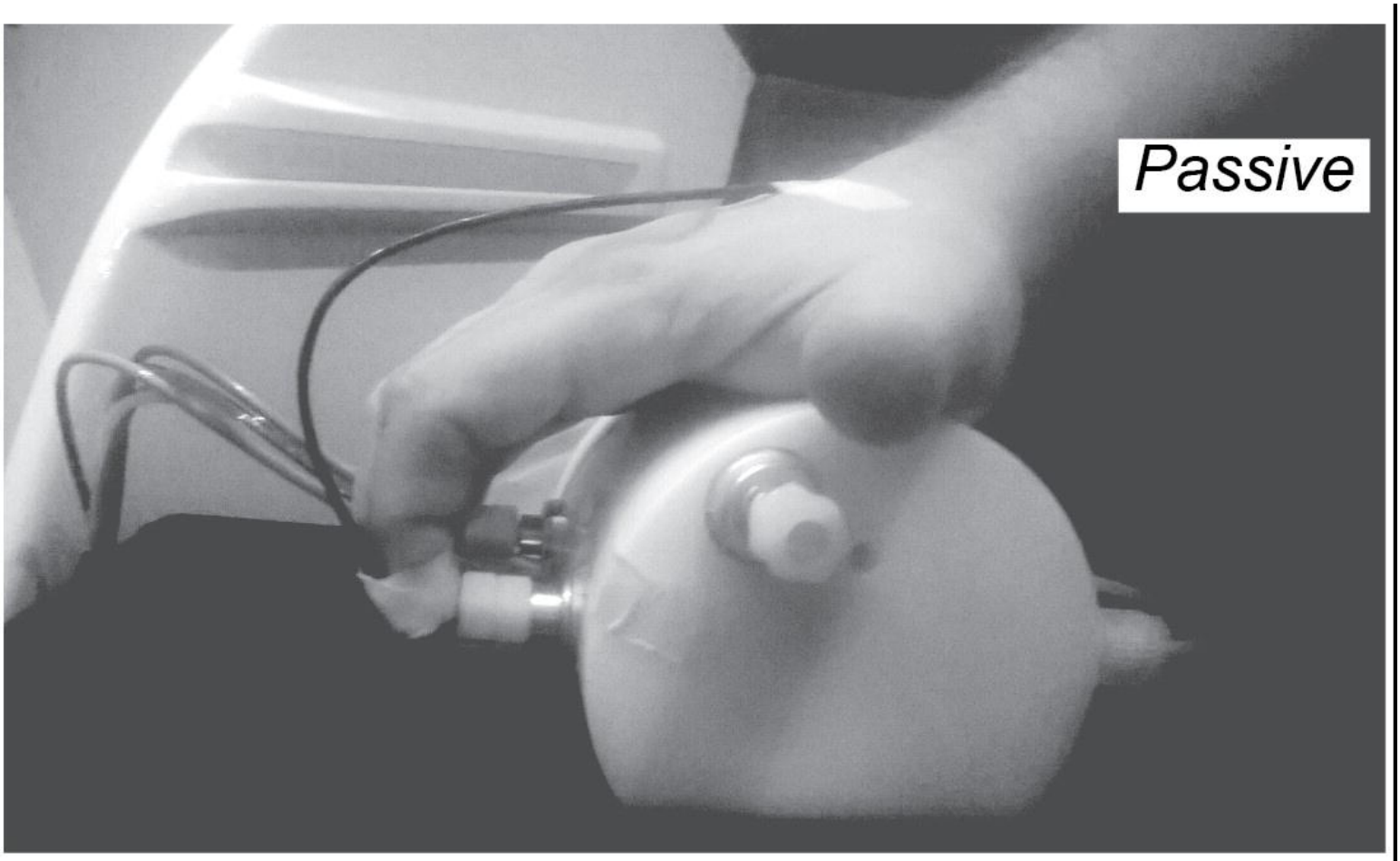

Active

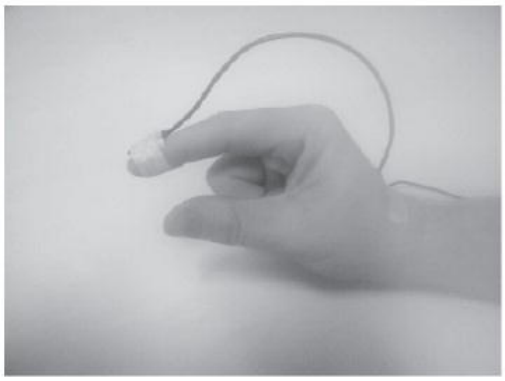

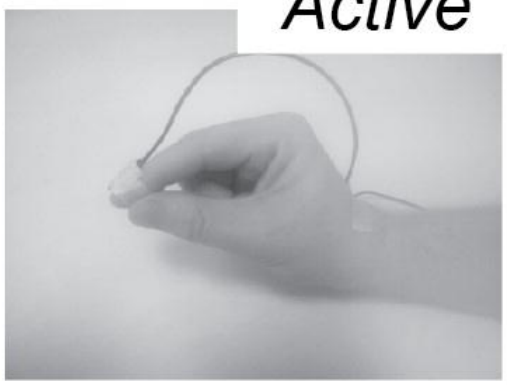

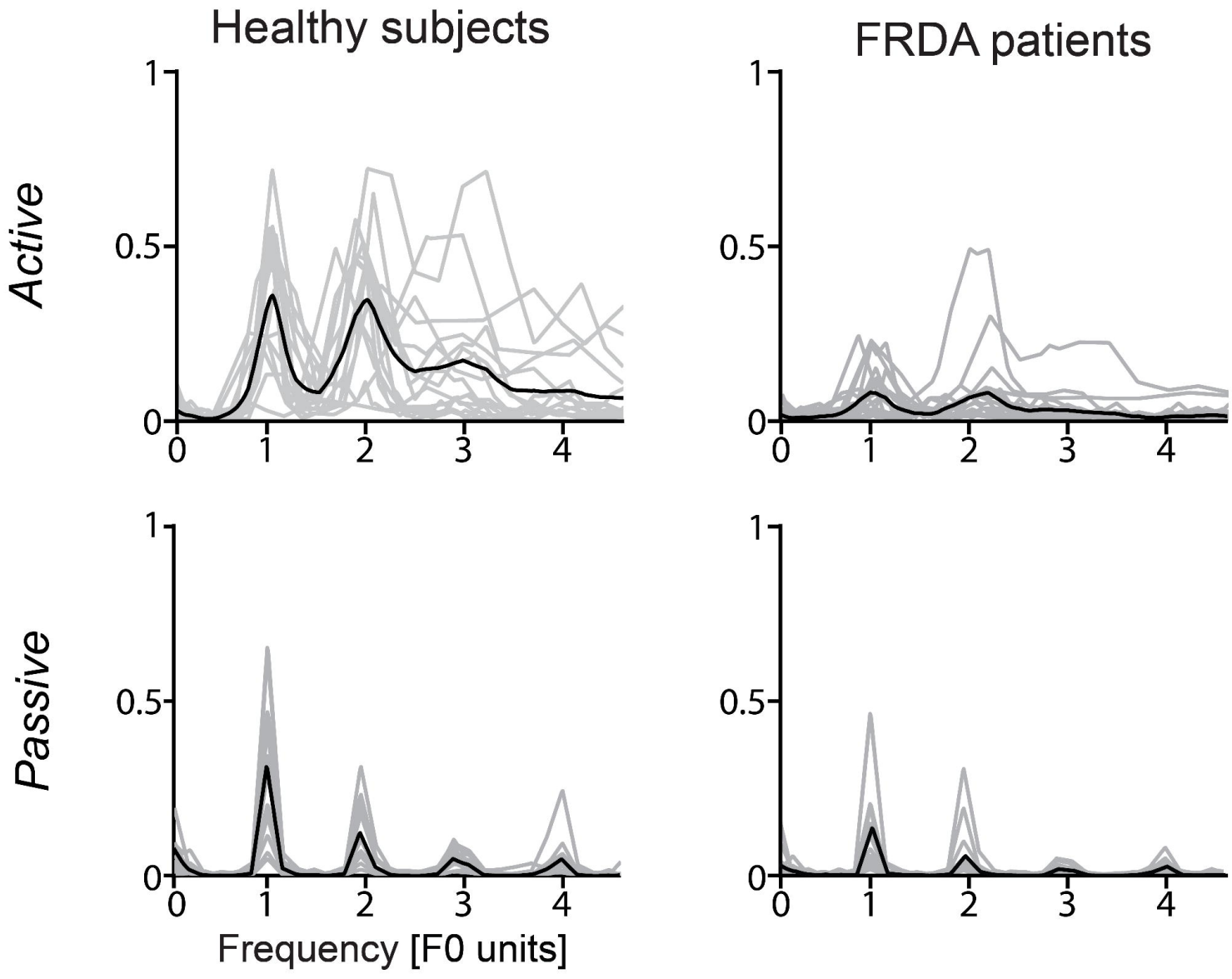
Healthy subjects
FRDA patients
Active
Passive
1
0.5
0
0
1
2
3
4
Frequency [F0 units]

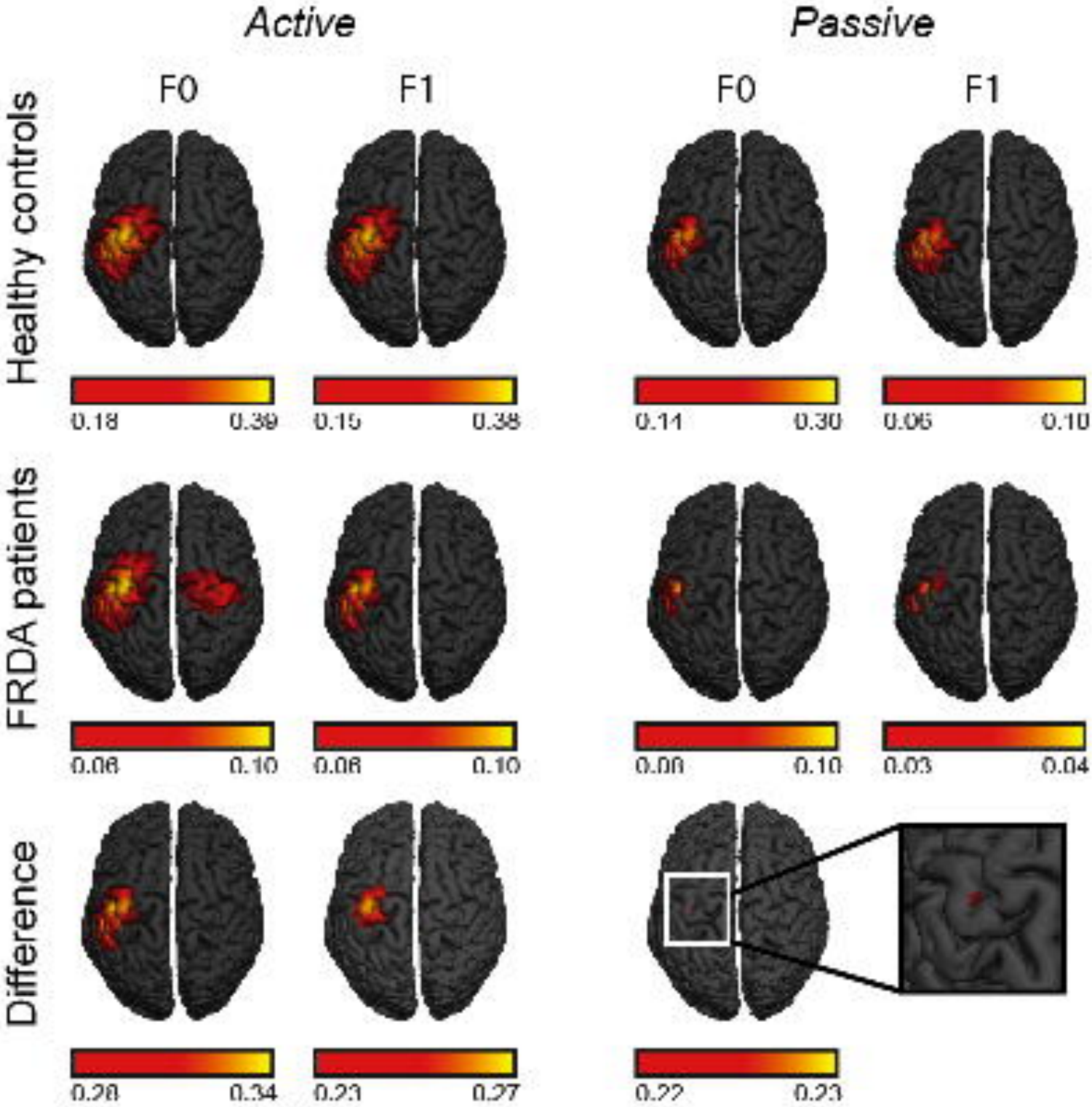
Active
Passive
F0
F1
F0
F1
Healthy controls
0.18
0.39
0.15
0.38
0.11
0.30
0.06
0.10
FRDA patients
0.08
0.10
0.08
0.10
0.00
0.10
0.03
0.04
Difference
0.28
0.34
0.23
0.27
0.22
0.23

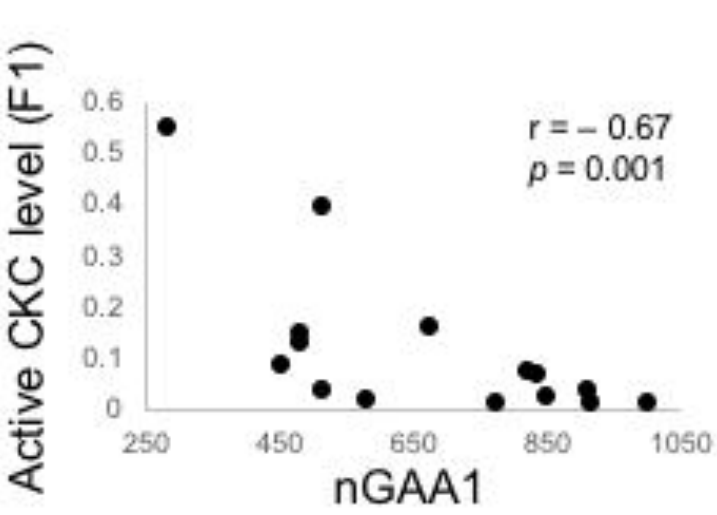
Active CKC level (F1)
0.6
0.5
0.4
0.3
0.2
0.1
0
250
450
650
850
1050
nGAA1
r = – 0.67
p = 0.001

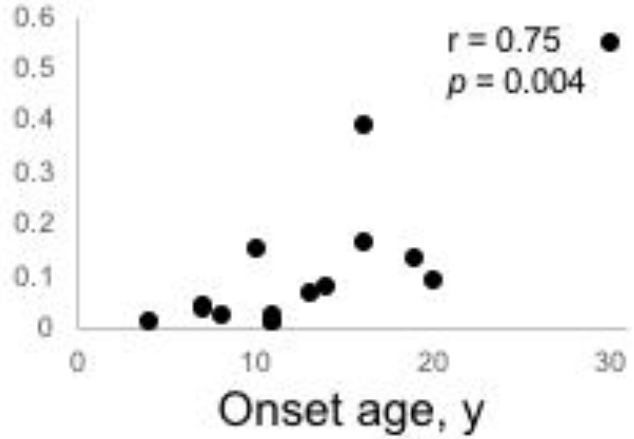
0.6
0.5
0.4
0.3
0.2
0.1
0
0
10
20
30
Onset age, y
r = 0.75
p = 0.004

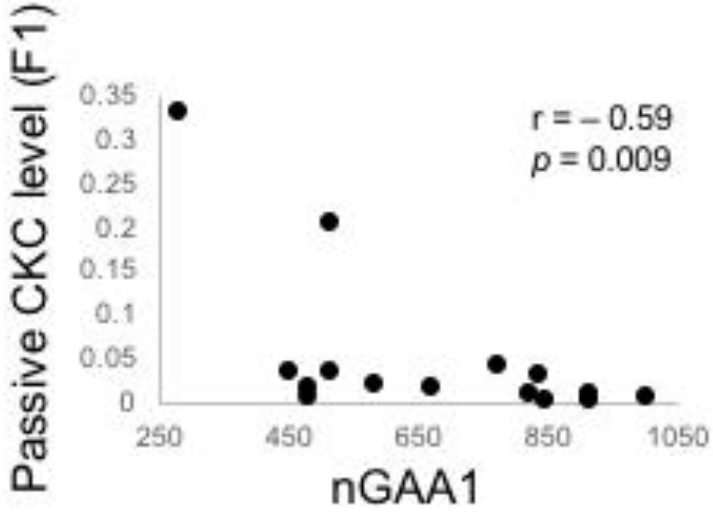
Passive CKC level (F1)
0.35
0.3
0.25
0.2
0.15
0.1
0.05
0
250
450
650
850
1050
nGAA1
r = – 0.59
p = 0.009